

Performance Analysis of Zero-Forcing Precoding in Multi-Cell One-Bit Massive MIMO Downlink

Qurrat-UI-Ain Nadeem and Anas Chaaban

School of Engineering, The University of British Columbia, Kelowna, Canada

Email: {qurrat.nadeem, anas.chaaban}@ubc.ca

Abstract—This work investigates the downlink performance of a multi-cell massive multiple-input multiple-output (MIMO) system that employs one-bit analog-to-digital converters (ADCs) and digital-to-analog converters (DACs) in the receiving and transmitting radio frequency (RF) chains at each base station (BS) in order to reduce the power consumption. We utilize Bussgang decomposition to derive the minimum mean squared error (MMSE) channel estimates at each BS based on the quantized received uplink training signals, and the asymptotic closed-form expressions of the achievable downlink rates under one-bit quantized zero-forcing (ZF) precoding implemented using the estimated channels. The derived expressions explicitly show the impact of quantization noise, thermal noise, pilot contamination, and interference, and are utilized to study the number of additional antennas needed at each BS of the one-bit MIMO system to perform as well as the conventional MIMO system. Numerical results verify our analysis, and reveal that despite needing more antennas to achieve the same sum average rate, the one-bit massive MIMO system is more energy-efficient than the conventional system, especially at high sampling frequencies.

Index Terms—Multi-cell massive MIMO, one-bit ADCs and DACs, Bussgang decomposition, ZF precoding, achievable rates.

I. INTRODUCTION

While the benefits of massive MIMO scale with the number of antennas M deployed at the base station (BS) [1], the power consumption and hardware cost associated with active components, like power amplifiers, analogue-to-digital converters (ADCs) and digital-to-analogue converters (DACs), that constitute the radio frequency (RF) chain connected to each antenna, also scale with M . Moreover the power consumption of ADCs and DACs increases exponentially with their resolution (in bits) and linearly with the sampling frequency [2], [3], with commercially available converters having 12 to 16 bits resolution consuming on the order of several watts [4]. The resolution of each ADC and DAC should therefore be limited to keep the power consumption at the massive MIMO BSs within tolerable levels.

Motivated by this discussion, we will consider the simplest possible scenario of a one-bit massive MIMO cellular network with BSs employing one-bit ADCs and DACs, that consist of a simple comparator and consume very low power [4], and characterize the downlink achievable rates under zero-forcing (ZF) precoding implemented using imperfect channel state information (CSI). While linear precoding schemes like maximum ratio transmission (MRT) and ZF have been shown to yield competitive performance to the optimal high-complexity dirty paper coding scheme in conventional massive MIMO

downlink where BSs employ full-resolution (FR) ADCs and DACs [5], very little has been reported on the impact of low-resolution ADCs and DACs on their performance.

In this context, the works in [6] and [7] studied the achievable rates, considering MRT precoding and imperfect CSI, in a single-cell one-bit massive MIMO and a cell-free one-bit massive MIMO system respectively. The authors in [3] derived asymptotic analytical expressions of the signal-to-quantization-plus-interference-plus-noise ratio (SQINR) and symbol error rate under one-bit quantized ZF precoding assuming perfect CSI and a single cell. Very recently, the authors in [8] considered a full-duplex massive MIMO cellular network with low-resolution ADCs and DACs at each BS, and derived spectral efficiency expressions under MRT precoding. To the best of our knowledge, the downlink performance of one-bit quantized ZF precoding under imperfect CSI has not been analyzed before in a single- or multi-cell setting.

In this work, we investigate the downlink sum average rate performance of a multi-cell one-bit massive MIMO system under ZF precoding and imperfect CSI. The analysis is based on Bussgang decomposition [9] that reformulates the non-linear quantizer operation as a statistically equivalent linear system. We first derive the minimum mean squared error (MMSE) channel estimates at each BS based on the received uplink training signals quantized by one-bit ADCs. Next the estimated CSI is used to implement ZF and generate the transmit signals, which are quantized by one-bit DACs. For this setting, we derive asymptotic closed-form expressions of the ergodic achievable downlink rates and study the extent of performance deterioration introduced by one-bit quantization. The derived expressions are used to study the ratio of the number of antennas at each BS in the one-bit cellular system to that at each BS in the conventional cellular system, required for both systems to achieve the same sum average rate. The ratio turns out to be 2.5 at low signal-to-noise ratio (SNR) values, while it is seen to decrease to one for any given SNR as the number of antennas grows large. Further, the numerical results reveal that despite needing more antennas to achieve the same sum rate, the one-bit system is more energy efficient than the conventional system at high sampling frequencies.

II. SYSTEM MODEL

We consider a multi-cell massive MIMO system consisting of $L > 1$ cells, with one M -antenna BS and $K \leq M$ single-

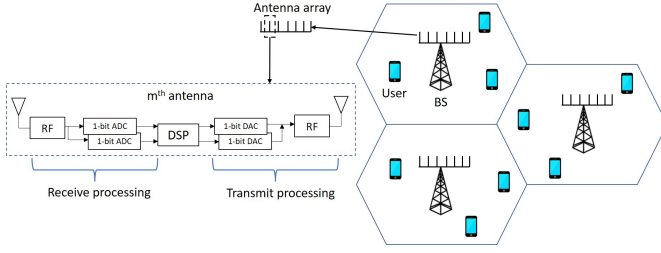


Fig. 1: Multi-cell one-bit massive MIMO system model.

antenna users in each cell. BS j wants to send information at rate R_{jk} to user k in cell j . To do this, it constructs codewords with symbols $s_{jk} \in \mathbb{C}$ and combines them in a transmit signal vector $\mathbf{x}_j \in \mathbb{C}^{M \times 1}$ given as $\mathbf{x}_j = \mathbf{W}_j \mathbf{s}_j$, where $\mathbf{W}_j \in \mathbb{C}^{M \times K}$ is the linear precoder that BS j applies to the vector of data symbols $\mathbf{s}_j = [s_{j1}, \dots, s_{jK}]^T \in \mathbb{C}^{K \times 1}$, with the latter satisfying $\mathbb{E}[\mathbf{s}_j \mathbf{s}_j^H] = \mathbf{I}_K$. The RF chain associated with each antenna at each BS is equipped with a pair of one-bit ADCs and DACs as shown in Fig. 1, one for each of the real and imaginary parts of the signal. The real and imaginary parts of the transmit signal \mathbf{x}_j are therefore converted into one bit representation (element-wise) based on the sign of each component, and then converted to analog using one-bit DACs. The final transmit signal from BS j is then written as

$$\tilde{\mathbf{x}}_j = Q(\mathbf{x}_j) = Q(\mathbf{W}_j \mathbf{s}_j), \quad (1)$$

where $Q(\cdot)$ is the one-bit quantization operation defined as

$$Q(\mathbf{a}) = \frac{1}{\sqrt{2}} \text{sign}(\Re(\mathbf{a})) + j \frac{1}{\sqrt{2}} \text{sign}(\Im(\mathbf{a})), \quad (2)$$

where $\Re(\mathbf{a})$ and $\Im(\mathbf{a})$ represent the real and imaginary parts of \mathbf{a} , and $\text{sign}(\cdot)$ is the sign of their arguments. The elements of $\tilde{\mathbf{x}}_j$ will belong to $\mathcal{R} = \frac{1}{\sqrt{2}}\{1+j, 1-j, -1+j, -1-j\}$.

The received signal at all users in cell j will be given as

$$\mathbf{y}_j = \sum_{l=1}^L \sqrt{\eta_l} \mathbf{H}_{lj}^H \tilde{\mathbf{x}}_l + \mathbf{n}_j, \quad (3)$$

where $\mathbf{H}_{lj} = [\mathbf{h}_{lj1}, \dots, \mathbf{h}_{ljK}] \in \mathbb{C}^{M \times K}$, $\mathbf{h}_{ljk} \in \mathbb{C}^{M \times 1}$ is the channel from BS l to user k in cell j , $\mathbf{n}_j = [n_{j1}, \dots, n_{jK}]^T \in \mathbb{C}^{K \times 1}$, and $n_{jk} \sim \mathcal{CN}(0, \sigma^2)$ is the received noise at user k in cell j . Moreover η_l is a normalization constant chosen to satisfy the average transmit power constraint at BS l as $\mathbb{E}[|\sqrt{\eta_l} \tilde{\mathbf{x}}_l|^2] = P_t$. Since $\mathbb{E}[|\tilde{\mathbf{x}}_l|^2] = M$ due to (2), we obtain $\eta_l = \frac{P_t}{M}$. The channel matrix \mathbf{H}_{lj} is modeled as

$$\mathbf{H}_{lj} = \mathbf{G}_{lj} \mathbf{D}_{lj}^{1/2}, \quad (4)$$

where $\mathbf{G}_{lj} = [\mathbf{g}_{lj1}, \dots, \mathbf{g}_{ljK}] \in \mathbb{C}^{M \times K}$ captures the small-scale fading, and $\mathbf{D}_{lj} = \text{diag}(\beta_{lj1}, \dots, \beta_{ljK}) \in \mathbb{C}^{K \times K}$ captures the large-scale fading. The entries of \mathbf{g}_{ljk} are independently and identically distributed (i.i.d.) complex Gaussian random variables, with zero mean and unit variance. The coefficients β_{ljk} represent the channel attenuation factors.

In the next section, we will outline the channel estimation done at BS j to obtain an estimate $\hat{\mathbf{H}}_{jj}$ of the channel matrix

$\mathbf{H}_{jj} = [\mathbf{h}_{jj1}, \dots, \mathbf{h}_{jjK}]$ to the users in its cell. This CSI is needed by the BS to implement precoding and construct the quantized transmit signal in (1). We consider ZF precoding in this work, which is well-known for its interference suppression capability, and is implemented using the estimated channels from the next section, as $\mathbf{W}_j = \hat{\mathbf{H}}_{jj} (\hat{\mathbf{H}}_{jj}^H \hat{\mathbf{H}}_{jj})^{-1}$.

III. UPLINK CHANNEL ESTIMATION

BS j obtains an estimate of $\mathbf{H}_{jj} = [\mathbf{h}_{jj1}, \dots, \mathbf{h}_{jjK}] \in \mathbb{C}^{M \times K}$ in an uplink training phase of length τ_p symbols at the start of each coherence block, in which the K users in cell j transmit mutually orthogonal pilot sequences, represented as $\Phi_j = [\phi_{j1}, \dots, \phi_{jK}] \in \mathbb{C}^{\tau_p \times K}$, satisfying $\Phi_j^H \Phi_j = \mathbf{I}_K$. The same set of pilot sequences is transmitted by the K users in every cell resulting in the channel estimate to be corrupted by pilot contamination. The received training signal $\mathbf{Y}_j^p \in \mathbb{C}^{M \times \tau_p}$ at BS j is given as $\mathbf{Y}_j^p = \sum_{l=1}^L \sqrt{\rho_p \tau_p} \mathbf{H}_{jl} \Phi_l^T + \mathbf{N}_j^p$, where ρ_p is the uplink SNR and $\mathbf{N}_j^p \in \mathbb{C}^{M \times \tau_p}$ has i.i.d. $\mathcal{CN}(0, \mathbf{I}_M)$ columns representing the noise. Next we write $\mathbf{y}_j^p = \text{vec}(\mathbf{Y}_j^p)$ as

$$\mathbf{y}_j^p = \sum_{l=1}^L \bar{\Phi}_l \mathbf{h}_{jl} + \mathbf{n}_j^p, \quad (5)$$

where $\bar{\Phi}_l = (\Phi_l \otimes \sqrt{\rho_p \tau_p} \mathbf{I}_M) \in \mathbb{C}^{M \tau_p \times M K}$, $\mathbf{h}_{jl} = \text{vec}(\mathbf{H}_{jl})$, $\mathbf{n}_j^p = \text{vec}(\mathbf{N}_j^p)$, and \otimes represents the Kronecker product.

The RF chain with each antenna at the BS is equipped with a pair of one-bit ADCs as shown in Fig. 1, that separately quantize the real and imaginary parts of the received signal to one-bit representation based on their sign. The quantized received training signal after one-bit ADCs is thus given as

$$\mathbf{r}_j^p = Q(\mathbf{y}_j^p) = Q\left(\sum_{l=1}^L \bar{\Phi}_l \mathbf{h}_{jl} + \mathbf{n}_j^p\right), \quad (6)$$

where $Q(\cdot)$ is defined in (2), and \mathbf{r}_j^p takes values from \mathcal{R} .

A. Bussgang Decomposition

Quantizing the training signal introduces a distortion $Q(\mathbf{y}_j^p) - \mathbf{r}_j^p$ that is correlated with the input \mathbf{y}_j^p to the ADCs. However, for Gaussian inputs, Bussgang's theorem [9] allows us to decompose the quantized signal into a linear function of the input to the quantizer and a distortion term that is uncorrelated with the input [4], [5]. The resulting linear representation of the non-linear quantization operation is statistically equivalent up to the second moments of the data and therefore facilitates ergodic rate analysis. Specifically, the Bussgang decomposition of \mathbf{r}_j^p in (6) is given as [4], [6]

$$\mathbf{r}_j^p = \mathbf{A}_j^p \mathbf{y}_j^p + \mathbf{q}_j^p, \quad (7)$$

where the matrix \mathbf{A}_j^p is the linear operator chosen to satisfy $\mathbb{E}[\mathbf{y}_j^p \mathbf{q}_j^{pH}] = \mathbf{0}$ as $\mathbf{A}_j^p = \mathbf{R}_{\mathbf{y}_j^p \mathbf{r}_j^p}^H \mathbf{R}_{\mathbf{y}_j^p \mathbf{y}_j^p}^{-1}$ [4], and \mathbf{q}_j^p is the uncorrelated quantizer noise. Further, for one-bit quantization and Gaussian inputs, $\mathbf{R}_{\mathbf{y}_j^p \mathbf{r}_j^p} = \sqrt{\frac{2}{\pi}} \mathbf{R}_{\mathbf{y}_j^p \mathbf{y}_j^p} \text{diag}(\mathbf{R}_{\mathbf{y}_j^p \mathbf{y}_j^p})^{-1/2}$ [9], [10, Chap. 10], which yields

$$\mathbf{A}_j^p = \sqrt{\frac{2}{\pi}} \text{diag}(\mathbf{R}_{\mathbf{y}_j^p \mathbf{y}_j^p})^{-1/2}, \quad (8)$$

where $\mathbf{R}_{\mathbf{y}_j^p \mathbf{y}_j^p}^H$ is the auto-covariance matrix of \mathbf{y}_j^p in (5), and $\text{diag}(\mathbf{C})$ denotes a diagonal square matrix with main-diagonal elements equal to those of \mathbf{C} . It is also useful to provide here the covariance matrix of \mathbf{q}_j^p , that can be written for a one-bit quantizer using the arcsin law as [3], [4], [7]

$$\mathbf{R}_{\mathbf{q}_j^p \mathbf{q}_j^p} = \frac{2}{\pi}(\arcsin(\mathbf{B}) + j \arcsin(\mathbf{C})) - \frac{2}{\pi}(\mathbf{B} + j\mathbf{C}), \quad (9)$$

where $\mathbf{B} = \text{diag}(\mathbf{R}_{\mathbf{y}_j^p \mathbf{y}_j^p})^{-1/2} \Re(\mathbf{R}_{\mathbf{y}_j^p \mathbf{y}_j^p}) \text{diag}(\mathbf{R}_{\mathbf{y}_j^p \mathbf{y}_j^p})^{-1/2}$ and $\mathbf{C} = \text{diag}(\mathbf{R}_{\mathbf{y}_j^p \mathbf{y}_j^p})^{-1/2} \Im(\mathbf{R}_{\mathbf{y}_j^p \mathbf{y}_j^p}) \text{diag}(\mathbf{R}_{\mathbf{y}_j^p \mathbf{y}_j^p})^{-1/2}$.

Next we utilize these results to complete the Bussgang decomposition of the quantized training signal in (6). We substitute (5) in (7) to write the Bussgang decomposition as

$$\mathbf{r}_j^p = \sum_{l=1}^L \mathbf{A}_j^p \bar{\Phi}_l \mathbf{h}_{jl} + \mathbf{A}_j^p \mathbf{n}_j^p + \mathbf{q}_j^p, \quad (10)$$

where to find \mathbf{A}_j^p using (8), we compute $\mathbf{R}_{\mathbf{y}_j^p \mathbf{y}_j^p}$ as $\mathbf{R}_{\mathbf{y}_j^p \mathbf{y}_j^p} = \mathbb{E}[\mathbf{y}_j^p \mathbf{y}_j^{pH}] = \sum_{l=1}^L \bar{\Phi}_l \bar{\mathbf{D}}_{jl} \bar{\Phi}_l^H + \mathbf{I}_{M\tau_p}$, where $\bar{\mathbf{D}}_{jl} = \mathbf{D}_{jl} \otimes \mathbf{I}_M \in \mathbb{C}^{MK \times MK}$ and \mathbf{D}_{jl} is defined in (4). The expression of $\mathbf{R}_{\mathbf{y}_j^p \mathbf{y}_j^p}$ indicates that the choice of $\bar{\Phi}_l$'s will affect the linear operator \mathbf{A}_j^p as well as the quantization noise. In order to obtain analytically tractable expressions for \mathbf{A}_j^p and the channel estimates, we consider $\tau_p = K$ and choose the K -dimensional identity matrix as each pilot matrix as done in [6], [7]. Note that investigating the impact of different choices of τ_p and $\bar{\Phi}_l$ on the quality of channel estimates under one-bit ADCs is an interesting research direction [4], but is beyond the scope of this work. Using $\bar{\Phi}_l = \mathbf{I}_K$, we obtain $\mathbf{R}_{\mathbf{y}_j^p \mathbf{y}_j^p} = \sum_{l=1}^L K \rho_p \bar{\mathbf{D}}_{jl} + \mathbf{I}_{MK}$, and compute \mathbf{A}_j^p as

$$\mathbf{A}_j^p = \bar{\mathbf{A}}_j^p \otimes \mathbf{I}_M, \quad (11)$$

where $\bar{\mathbf{A}}_j^p$ is a diagonal matrix with entries $[\bar{\mathbf{A}}_j^p]_{kk} = \bar{a}_{jk} = \sqrt{\frac{2}{\pi(\sum_{l=1}^L K \rho_p \beta_{jlk} + 1)}}$. Further using $\mathbf{R}_{\mathbf{y}_j^p \mathbf{y}_j^p}$ in (9), we have

$$\mathbf{R}_{\mathbf{q}_j^p \mathbf{q}_j^p} = \left(1 - \frac{2}{\pi}\right) \mathbf{I}_{MK}. \quad (12)$$

This completes the Bussgang decomposition of the quantized training signal \mathbf{r}_j^p , with (10) being the statistically equivalent linear representation of (6) under the definition of \mathbf{A}_j^p in (11).

B. MMSE Estimation

The MMSE estimate of the channel vector \mathbf{h}_{jj} at BS j based on the quantized training signal \mathbf{r}_j^p is presented next.

Lemma 1: BS j estimates $\mathbf{h}_{jj} = [\mathbf{h}_{jj1}^T, \dots, \mathbf{h}_{jjK}^T]^T \in \mathbb{C}^{MK \times 1}$ using the quantized training signal in (10) as

$$\hat{\mathbf{h}}_{jj} = \sqrt{\rho_p K} \bar{\mathbf{D}}_{jj} \mathbf{A}_j^{pH} \mathbf{r}_j^p \quad (13)$$

where $\bar{\mathbf{D}}_{jj} = \mathbf{D}_{jj} \otimes \mathbf{I}_M$, and \mathbf{A}_j^p is defined in (11).

Proof: The proof follows by applying the standard definition of the MMSE estimate [7, equation (14)]. ■

Although the channel estimate in (13) is not Gaussian in general due to the quantization noise \mathbf{q}_j^p that appears in \mathbf{r}_j^p , we can approximate it as Gaussian using the Cramer's central limit theorem assuming M is sufficiently large [4], [6], [11]. Thus we consider the channel estimate to be distributed as

$\hat{\mathbf{h}}_{jj} \sim \mathcal{CN}(\mathbf{0}, \mathbf{R}_{\hat{\mathbf{h}}_{jj} \hat{\mathbf{h}}_{jj}})$, where the covariance matrix of the estimate $\mathbf{R}_{\hat{\mathbf{h}}_{jj} \hat{\mathbf{h}}_{jj}}$ is given as $\mathbf{R}_{\hat{\mathbf{h}}_{jj} \hat{\mathbf{h}}_{jj}} = \mathbf{T}_{jj} \otimes \mathbf{I}_M$, where \mathbf{T}_{jj} is a diagonal matrix with entries

$$[\mathbf{T}_{jj}]_{k,k} = t_{jjk} = \frac{2\beta_{jjk}^2 \rho_p K}{\pi(\sum_{l=1}^L K \rho_p \beta_{jlk} + 1)}. \quad (14)$$

Under orthogonality property of MMSE estimate, the channel estimate and the estimation error defined as $\tilde{\mathbf{h}}_{jj} = \mathbf{h}_{jj} - \hat{\mathbf{h}}_{jj}$, are uncorrelated, with $\tilde{\mathbf{h}}_{jj} \sim \mathcal{CN}(\mathbf{0}, \bar{\mathbf{D}}_{jj} - \mathbf{R}_{\hat{\mathbf{h}}_{jj} \hat{\mathbf{h}}_{jj}})$.

To facilitate the analysis, we can extract the estimate of the channel from BS j to user k in cell j from (13) as $\hat{\mathbf{h}}_{jjk} = \sqrt{\rho_p K} \beta_{jjk} \bar{a}_{jk} \mathbf{r}_{jk}^p$, where $\mathbf{r}_{jk}^p = \sum_{l=1}^L \sqrt{\rho_p K} \bar{a}_{jk} \mathbf{h}_{jlk} + \bar{a}_{jk} \mathbf{n}_{jk}^p + \mathbf{q}_{jk}^p$, and \mathbf{n}_{jk}^p and \mathbf{q}_{jk}^p are vectors of $(k-1)M+1$ to kM entries of \mathbf{n}_j^p and \mathbf{q}_j^p respectively. It then follows that $\hat{\mathbf{h}}_{jjk} \sim \mathcal{CN}(\mathbf{0}, t_{jjk} \mathbf{I}_M)$ where t_{jjk} is defined in (14), and $\tilde{\mathbf{h}}_{jjk} \sim \mathcal{CN}(\mathbf{0}, \bar{t}_{jjk} \mathbf{I}_M)$, where $\bar{t}_{jjk} = \beta_{jjk} - t_{jjk}$.

Corollary 1: When BSs have full-resolution (FR) ADCs, the estimate of the channel from BS j to user k in cell j is

$$\hat{\mathbf{h}}_{jjk}^{\text{FR}} = \sqrt{\rho_p K} \beta_{jjk} \mathbf{r}_{jk}^p \quad (15)$$

where $\mathbf{r}_{jk}^p = \sum_{l=1}^L \sqrt{\rho_p K} \mathbf{h}_{jlk} + \mathbf{n}_{jk}^p$. It follows that $\hat{\mathbf{h}}_{jjk}^{\text{FR}} \sim \mathcal{CN}(\mathbf{0}, t_{jjk}^{\text{FR}} \mathbf{I}_M)$ where $t_{jjk}^{\text{FR}} = \frac{\beta_{jjk}^2 \rho_p K}{\sum_{l=1}^L K \rho_p \beta_{jlk} + 1}$, and $\tilde{\mathbf{h}}_{jjk}^{\text{FR}} \sim \mathcal{CN}(\mathbf{0}, \bar{t}_{jjk}^{\text{FR}} \mathbf{I}_M)$ where $\bar{t}_{jjk}^{\text{FR}} = \beta_{jjk} - t_{jjk}^{\text{FR}}$.

Proof: The corollary follows from [1, Sec. II-C]. ■

It is straightforward to see that $t_{jjk} = \frac{2}{\pi} t_{jjk}^{\text{FR}}$, and therefore $\bar{t}_{jjk} > \bar{t}_{jjk}^{\text{FR}}$. The use of one-bit ADCs in the RF chains at the BSs therefore deteriorates the accuracy of channel estimation, which will decrease the system performance.

IV. DOWNLINK ACHIEVABLE RATE ANALYSIS

In this section, we analyze the ergodic achievable downlink rates under one-bit quantized ZF precoding.

A. Bussgang Decomposition of Transmit Signal

We again utilize Bussgang decomposition to obtain a linear representation of the quantized transmit signal in (1). Even though the entries of $\mathbf{x}_j = \mathbf{W}_j \mathbf{s}_j$, which is the input to the quantizer in (1), are not necessarily Gaussian, each element of \mathbf{x}_j is formed as a result of the linear mixture of K i.i.d. elements of the vector \mathbf{s}_j and can be approximated as Gaussian using Cramer's central limit theorem [11] for large K [3], [6]. We therefore apply Bussgang theorem to decompose the quantized signal in (1) into a linear function of the input \mathbf{x}_j to the quantizer and a quantization noise term \mathbf{q}_j that is uncorrelated with input as [3], [6], [5, Theorem 2]

$$\tilde{\mathbf{x}}_j = Q(\mathbf{x}_j) = \mathbf{A}_j \mathbf{x}_j + \mathbf{q}_j, \quad (16)$$

where $\mathbf{A}_j = \sqrt{\frac{2}{\pi}} \text{diag}(\mathbf{R}_{\mathbf{x}_j \mathbf{x}_j})^{-1/2}$, and $\mathbf{R}_{\mathbf{x}_j \mathbf{x}_j} = \mathbb{E}_{\mathbf{s}_j}[\mathbf{x}_j \mathbf{x}_j^H] = \mathbb{E}_{\mathbf{s}_j}[\mathbf{W}_j \mathbf{s}_j \mathbf{s}_j^H \mathbf{W}_j^H] = \mathbf{W}_j \mathbf{W}_j^H$ [5, Corollary 3]. Moreover using the arcsin law, the autocovariance matrix of \mathbf{q}_j can be obtained as $\mathbf{R}_{\mathbf{q}_j \mathbf{q}_j} = \frac{2}{\pi}(\arcsin(\bar{\mathbf{B}}) + j \arcsin(\bar{\mathbf{C}})) - \frac{2}{\pi}(\bar{\mathbf{B}} + j\bar{\mathbf{C}})$, where $\bar{\mathbf{B}} = \text{diag}(\mathbf{R}_{\mathbf{x}_j \mathbf{x}_j})^{-1/2} \Re(\mathbf{R}_{\mathbf{x}_j \mathbf{x}_j}) \text{diag}(\mathbf{R}_{\mathbf{x}_j \mathbf{x}_j})^{-1/2}$ and $\bar{\mathbf{C}} = \text{diag}(\mathbf{R}_{\mathbf{x}_j \mathbf{x}_j})^{-1/2} \Im(\mathbf{R}_{\mathbf{x}_j \mathbf{x}_j}) \text{diag}(\mathbf{R}_{\mathbf{x}_j \mathbf{x}_j})^{-1/2}$ [5], [7]. Next we approximate $\mathbf{R}_{\mathbf{x}_j \mathbf{x}_j} = \mathbf{W}_j \mathbf{W}_j^H$ as a deterministic

quantity under ZF precoding and find \mathbf{A}_j to complete the Bussgang decomposition in (16).

Lemma 2: Under ZF precoding, the Bussgang decomposition of the quantized transmit signal in (1) for large (M, K) values such that the ratio $M/K = c < \infty$, is given as

$$\tilde{\mathbf{x}}_j = \mathbf{A}_j \mathbf{W}_j \mathbf{s}_j + \mathbf{q}_j \quad (17)$$

where $\mathbf{A}_j = \sqrt{\frac{2K(c-1)^2}{\pi\zeta_j}} \mathbf{I}_M$, $\mathbf{R}_{\mathbf{q}_j \mathbf{q}_j} = (1 - \frac{2}{\pi}) \mathbf{I}_M$, and $\zeta_j = \frac{1}{K} \sum_{k=1}^K \frac{1}{t_{jjk}}$, where t_{jjk} is defined in Lemma 1.

Proof: We utilize [3, (34)] to obtain an asymptotic approximation for $\mathbf{R}_{\mathbf{x}_j \mathbf{x}_j} = \mathbf{W}_j \mathbf{W}_j^H = \hat{\mathbf{H}}_j (\hat{\mathbf{H}}_j^H \hat{\mathbf{H}}_j)^{-2} \hat{\mathbf{H}}_j^H$ under ZF precoding, which is very tight for moderate system sizes as well, and use it to compute \mathbf{A}_j and $\mathbf{R}_{\mathbf{q}_j \mathbf{q}_j}$. ■

B. Achievable Rates

We now outline the achievable rates at the users and develop closed-form expressions for them under one-bit and conventional massive MIMO settings. To this end, we utilize the decomposition of $\tilde{\mathbf{x}}_j$ in (17) to write the received signal at user k in cell j using (3) as $y_{jk} = \sum_{l=1}^L \sqrt{\eta_l} \mathbf{h}_{ljk}^H \mathbf{A}_l \mathbf{W}_l \mathbf{s}_l + \sum_{l=1}^L \sqrt{\eta_l} \mathbf{h}_{ljk}^H \mathbf{q}_l + n_{jk}$. Since the users do not have channel estimates, we provide an ergodic achievable rate based on the technique developed in [12], that exploits the fact that the effective channel $\mathbf{h}_{ljk}^H \mathbf{A}_j \mathbf{w}_{jk}$ of user k in cell j approaches its average value $\mathbb{E}[\mathbf{h}_{ljk}^H \mathbf{A}_j \mathbf{w}_{jk}]$ as M grows large due to channel hardening. Hence, asymptotically it is sufficient for each user to only have statistical CSI (i.e. knowledge of $\mathbb{E}[\mathbf{h}_{ljk}^H \mathbf{A}_j \mathbf{w}_{jk}]$). The main idea then is to decompose y_{jk} as

$$\begin{aligned} y_{jk} = & \underbrace{\sqrt{\eta_j} \mathbb{E}[\mathbf{h}_{ljk}^H \mathbf{A}_j \mathbf{w}_{jk}] \mathbf{s}_{jk}}_{\text{Desired signal}} + \underbrace{\sqrt{\eta_j} (\mathbf{h}_{ljk}^H \mathbf{A}_j \mathbf{w}_{jk} - \mathbb{E}[\mathbf{h}_{ljk}^H \mathbf{A}_j \mathbf{w}_{jk}]) \mathbf{s}_{jk}}_{\text{Channel gain uncertainty}} \\ & + \underbrace{\sum_{(l,m) \neq (j,k)} \sqrt{\eta_l} \mathbf{h}_{ljk}^H \mathbf{A}_l \mathbf{w}_{lm} \mathbf{s}_{lm}}_{\text{Inter-user interference}} + \underbrace{\sum_{l=1}^L \sqrt{\eta_l} \mathbf{h}_{ljk}^H \mathbf{q}_l}_{\text{Quantization noise}} + \underbrace{n_{jk}}_{\text{Thermal noise}} \quad (18) \end{aligned}$$

and assume that the average effective channel $\mathbb{E}[\mathbf{h}_{ljk}^H \mathbf{A}_j \mathbf{w}_{jk}]$ can be perfectly learned at user k in cell j . The sum of the last four terms in (18) is considered as effective additive noise. Treating this noise as uncorrelated Gaussian as a worst-case, user k in cell j can achieve the ergodic rate [12, Theorem 1]

$$R_{jk} = \log_2(1 + \gamma_{jk}) \quad (19)$$

where γ_{jk} is the associated SQINR obtained using (18) as

$$\gamma_{jk} = \frac{\text{DS}_{jk}}{\text{CU}_{jk} + \text{QN}_{jk} + \text{IUI}_{jk} + \text{TN}_{jk}} \quad (20)$$

where $\text{DS}_{jk} = \eta_j |\mathbb{E}[\mathbf{h}_{ljk}^H \mathbf{A}_j \mathbf{w}_{jk}]|^2$ is the power of the average desired signal, $\text{CU}_{jk} = \eta_j \text{Var}[\mathbf{h}_{ljk}^H \mathbf{A}_j \mathbf{w}_{jk}]$ is the average channel gain uncertainty power, $\text{QN}_{jk} = \sum_{l=1}^L \eta_l \mathbb{E}[\mathbf{h}_{ljk}^H \mathbf{C}_{\mathbf{q}_l \mathbf{q}_l} \mathbf{h}_{ljk}]$ is the average quantization noise power, $\text{IUI}_{jk} = \sum_{(l,m) \neq (j,k)} \eta_l \mathbb{E}[|\mathbf{h}_{ljk}^H \mathbf{A}_l \mathbf{w}_{lm}|^2]$ is the average inter-user interference power, and $\text{TN}_{jk} = \sigma^2$ is the thermal noise power. The sum average rate is then given as

$$R_{\text{sum}} = \sum_{j=1}^L \sum_{k=1}^K R_{jk}. \quad (21)$$

Note that these definitions of the ergodic achievable downlink rate in (19) and SQINR in (20) will be used for performance evaluation based on Monte-Carlo simulations in Sec. V. To yield explicit theoretical insights into the impact of one-bit quantization on the sum average rate, we derive the expectations in (20) in closed-form, resulting in an analytical expression for (19) that is presented in the following theorem.

Theorem 1: Consider a one-bit massive MIMO cellular network with BSs equipped with one-bit ADCs and DACs. Then under ZF precoding and large (M, K) values such that $\frac{M}{K} = c$ is finite, the ergodic achievable rate in (19) and SQINR in (20) at user k in cell j are given in closed-form as

$$R_{jk}^{\text{one}} = \log_2(1 + \gamma_{jk}^{\text{one}}), \quad (22)$$

$$\gamma_{jk}^{\text{one}} = \frac{1}{\overline{\text{CU}}_{jk}^{\text{one}} + \overline{\text{QN}}_{jk}^{\text{one}} + \overline{\text{IUI}}_{jk}^{\text{one}} + \overline{\text{PC}}_{jk}^{\text{one}} + \overline{\text{TN}}_{jk}^{\text{one}}}, \quad (23)$$

where $\overline{\text{CU}}_{jk}^{\text{one}} = \frac{\beta_{jjk} - t_{jjk}}{(M-K)t_{jjk}}$ is the normalized average channel gain uncertainty power, $\overline{\text{QN}}_{jk}^{\text{one}} = \sum_{l=1}^L (1 - \frac{2}{\pi}) \frac{\pi M \beta_{ljk} \zeta_j}{2K(c-1)^2}$ is the normalized average quantization noise power, $\overline{\text{IUI}}_{jk}^{\text{one}} = \sum_{m \neq k} \frac{(\beta_{jjk} - t_{jjk})}{t_{jjm}(M-K)} + \sum_{l \neq j} \sum_{m \neq k} \frac{\zeta_l \beta_{ljk}}{\zeta_l t_{lkm}(M-K)} + \sum_{l \neq j} \frac{\zeta_j \beta_{ljk}}{\zeta_l t_{ljk}(M-K)} \left(1 - \frac{t_{ljk} \beta_{ljk}}{\beta_{ljk}^2}\right)$ is the normalized average inter-user interference power, $\overline{\text{PC}}_{jk}^{\text{one}} = \sum_{l \neq j} \frac{\zeta_j \beta_{ljk}^2}{\zeta_l \beta_{ljk}^2}$ is the normalized average pilot contamination power, and $\overline{\text{TN}}_{jk}^{\text{one}} = \frac{\pi M \sigma^2 \zeta_j}{2K P_t (c-1)^2}$ is the normalized average thermal noise power (all normalized by the power of the average desired signal).

Proof: The proof follows by using $\mathbf{A}_j = \sqrt{\frac{2K(c-1)^2}{\pi\zeta_j}} \mathbf{I}_M$, $\eta_j = \frac{P_t}{M}$, the channel in (4), the estimates in Lemma 1, $\mathbf{H}_{jj}^H \mathbf{W}_j = \mathbf{I}_K + \hat{\mathbf{H}}_{jj}^H \mathbf{W}_j$, and the observation that the estimates of the channels at BS l to user k in cell l and to user k in cell j are correlated due to pilot contamination, to compute the terms in (20). All terms in the denominator of the resulting expression are divided by the expression of DS_{jk} , and represented as $\overline{\text{CU}}_{jk}$, $\overline{\text{QN}}_{jk}$, $\overline{\text{IUI}}_{jk}$, $\overline{\text{PC}}_{jk}$, and $\overline{\text{TN}}_{jk}$. ■

Next we present the closed-form expression of the achievable rate in (19) for the conventional massive MIMO network.

Corollary 2: Consider the conventional massive MIMO cellular network employing FR ADCs and DACs. Then under ZF precoding, the ergodic rate R_{jk} in (19) and the associated SINR γ_{jk} of user k in cell j are given in closed-form as

$$R_{jk}^{\text{conv}} = \log_2(1 + \gamma_{jk}^{\text{conv}}), \quad (24)$$

$$\gamma_{jk}^{\text{conv}} = \frac{1}{\overline{\text{CU}}_{jk}^{\text{conv}} + \overline{\text{IUI}}_{jk}^{\text{conv}} + \overline{\text{PC}}_{jk}^{\text{conv}} + \overline{\text{TN}}_{jk}^{\text{conv}}}, \quad (25)$$

where $\overline{\text{CU}}_{jk}^{\text{conv}} = \frac{\beta_{jjk} - t_{jjk}^{\text{FR}}}{(M-K)t_{jjk}^{\text{FR}}}$, $\overline{\text{IUI}}_{jk}^{\text{conv}} = \sum_{m \neq k} \frac{(\beta_{jjk} - t_{jjk}^{\text{FR}})}{t_{jjm}^{\text{FR}}(M-K)} + \sum_{l \neq j} \sum_{m \neq k} \frac{\zeta_l^{\text{FR}} \beta_{ljk}}{\zeta_l^{\text{FR}} t_{lkm}^{\text{FR}}(M-K)} + \sum_{l \neq j} \frac{\zeta_j^{\text{FR}} \beta_{ljk}}{\zeta_l^{\text{FR}} t_{ljk}^{\text{FR}}(M-K)} \left(1 - \frac{t_{ljk}^{\text{FR}} \beta_{ljk}}{\beta_{ljk}^2}\right)$, $\overline{\text{PC}}_{jk}^{\text{conv}} = \sum_{l \neq j} \frac{\zeta_j^{\text{FR}} \beta_{ljk}^2}{\zeta_l^{\text{FR}} \beta_{ljk}^2}$, and $\overline{\text{TN}}_{jk}^{\text{conv}} = \frac{\sigma^2 K \zeta_j^{\text{FR}}}{P_t (M-K)}$, with t_{jjk}^{FR} defined in Corollary 1 and $\zeta_j^{\text{FR}} = \frac{1}{K} \sum_{k=1}^K \frac{1}{t_{jjk}^{\text{FR}}}$.

Comparing the results in Theorem 1 and Corollary 2, we see that using one-bit ADCs and DACs not only in-

roduces a quantization noise term $\overline{\text{QN}}_{jk}$ in γ_{jk} , but it also increases the noise and interference terms as $\frac{\overline{\text{TN}}_{jk}^{\text{one}}}{\overline{\text{TN}}_{jk}^{\text{conv}}} = \frac{\pi^2 M}{4K(c-1)} \approx \frac{\pi^2}{4}$, $\frac{\overline{\text{CU}}_{jk}^{\text{one}}}{\overline{\text{CU}}_{jk}^{\text{conv}}} = \frac{\pi}{2} \left(\frac{\beta_{jjk} - \frac{2}{\pi} \iota_{jjk}^{\text{FR}}}{\beta_{jjk} - \iota_{jjk}^{\text{FR}}} \right) > \frac{\pi}{2}$, and $\frac{\overline{\text{IU}}_{jk}^{\text{one}}}{\overline{\text{IU}}_{jk}^{\text{conv}}} = \frac{\pi}{2} \frac{(M-K)\overline{\text{IU}}_{jk}^{\text{conv}} + \sum_{m \neq k}^K (1 - \frac{2}{\pi}) \frac{\iota_{jjm}^{\text{FR}}}{\beta_{jjm}} + \sum_{l \neq j} (1 - \frac{2}{\pi}) \frac{c_{jl}^{\text{FR}} \beta_{ljk}^2}{\zeta_l^{\text{FR}} \beta_{llk}^2}}{(M-K)\overline{\text{IU}}_{jk}^{\text{conv}}} > \frac{\pi}{2}$, resulting in reduced rates under the setting of Theorem 1. Interestingly, pilot contamination to desired signal energy ratio is unaffected by one-bit quantization as $\overline{\text{PC}}_{jk}^{\text{one}} = \overline{\text{PC}}_{jk}^{\text{conv}}$.

Finally we show that the performance under both settings considered in Theorem 1 and Corollary 2 converges to the same limit as $M \rightarrow \infty$ while the other variables are fixed.

Corollary 3: The ergodic achievable downlink rates for both settings above converge as $R_{jk} \xrightarrow{M \rightarrow \infty} R_{jk}^{\infty}$, where $R_{jk}^{\infty} = \log_2 \left(1 + \frac{1}{\overline{\text{PC}}_{jk}} \right)$, $\overline{\text{PC}}_{jk} = \sum_{l \neq j}^L \frac{\zeta_j \beta_{ljk}^2}{\zeta_l \beta_{llk}^2}$ represents the average pilot contamination power to average desired signal power ratio, $\zeta_j = \sum_{k=1}^K \frac{1}{c_{jjk}}$, and $c_{jjk} = \frac{\beta_{jjk}^2}{\sum_{l=1}^L K \rho_p \beta_{jlk} + 1}$.

Therefore the effects of channel uncertainty, quantization noise, thermal noise, and interference vanish as $M \rightarrow \infty$, while pilot contamination remains the only performance limitation under both settings. This also implies that by using a larger number of antennas equipped with low power one-bit ADCs and DACs in the one-bit massive MIMO network, we can compensate for quantization noise and approach the performance of conventional massive MIMO as studied next.

C. How Many More Antennas are Needed in One-Bit MIMO?

We denote the number of antennas at each BS and the achievable sum average rate of the one-bit and conventional cellular systems as $(M^{\text{one}}, R_{\text{sum}}^{\text{one}})$ and $(M^{\text{conv}}, R_{\text{sum}}^{\text{conv}})$ respectively. Our goal in this section is to study the ratio $\kappa = \frac{M^{\text{one}}}{M^{\text{conv}}}$ required for the one-bit massive MIMO system to achieve the same sum average rate as the conventional massive MIMO system with M^{conv} antennas. In the low SNR regime, i.e. for small values of $\frac{P_t}{\sigma^2}$, we obtain κ explicitly as follows.

Corollary 4: At low SNR values, the ratio κ required for one-bit massive MIMO cellular system to achieve the sum average rate of conventional massive MIMO cellular system with M^{conv} antennas at each BS is $\kappa = \frac{M^{\text{one}}}{M^{\text{conv}}} \approx \frac{\pi^2}{4} \approx 2.5$.

Proof: The proof follows by simplifying (23) and (25) for small $\frac{P_t}{\sigma^2}$, and finding κ to guarantee $R_{\text{sum}}^{\text{one}} = R_{\text{sum}}^{\text{conv}}$. ■

While we can not get a closed-form expression for κ at moderate to high SNR values, we will find it numerically in the simulations through a simple search over the interval $[1, \infty)$ to guarantee that $R_{\text{sum}}^{\text{one}} = R_{\text{sum}}^{\text{conv}}$, and will observe it to be > 2.5 for moderate values of M^{conv} . This is because as the SNR increases, the quantization noise term comes into play in γ_{jk}^{one} , and the channel gain uncertainty and inter-user interference terms also become dominant and are significantly increased under one-bit implementation. This results in an overall larger decrease in achievable sum average rate in the one-bit MIMO setting, requiring a higher κ to compensate for it and achieve $R_{\text{sum}}^{\text{conv}}$. However as M^{conv} increases to larger numbers, κ decreases and approaches one as outlined next.

Remark 1: As $M^{\text{conv}} \rightarrow \infty$, $\kappa = M^{\text{one}}/M^{\text{conv}} \rightarrow 1$ since $R_{\text{sum}}^{\text{one}}$ and $R_{\text{sum}}^{\text{conv}}$ both converge to $\sum_{l=1}^L \sum_{j=1}^K R_{jk}^{\infty}$ as shown in Corollary 3. Therefore the impact of one-bit quantization becomes smaller as we work with larger antenna arrays.

V. SIMULATION RESULTS

We consider $L = 4$ cells (unless otherwise stated in the figure) with Cartesian coordinates of the BSs set as $(0, 0, 0)$, $(525, 0, 0)$, $(0, 525, 0)$, and $(525, 525, 0)$ (in metres). The BS in each cell has M antennas serving K users distributed uniformly on a circle of radius 250 metres around it [1]. Moreover $\sigma^2 = -80\text{dBm}$, $\rho_p = \frac{1}{\sigma^2}$, $\beta_{jlk} = \frac{10^{-3}}{d_{jlk}^{\alpha}}$, $\alpha = 3$, and d_{jlk} is the distance between BS j and user k in cell l .

We first validate the closed-form expressions of the achievable rates in Fig. 2, where we plot the sum ergodic rate per user given as $\frac{1}{K} R_{\text{sum}}$. The theoretical (Th) results are plotted using the expressions of R_{jk} in Theorem 1 and Corollary 2 for the one-bit and conventional massive MIMO scenarios respectively. The Monte-Carlo (MC) simulated curves are plotted by computing R_{jk} in (19) for both scenarios. A perfect match between the MC simulated and theoretical results can be seen, even for moderate system dimensions. As expected, there is a performance degradation when we use one-bit ADCs and DACs, with the decrease being more significant for a smaller number of cells. This is because the intra-cell interference becomes noticeable when compared to inter-cell interference for $L = 2$, and is more effectively combated by conventional ZF than one-bit quantized ZF precoding.

Next in Fig. 3, we plot the sum average rate per user against M for both one-bit and conventional massive MIMO systems. For $M = 800$, one-bit quantized and conventional ZF precoding are seen to achieve 73% and 88% of the asymptotic sum average rate outlined in Corollary 3. The performance gap between the two settings decreases with M implying that the impact of quantization becomes increasingly small as $M \rightarrow \infty$. Further to achieve the rate of 3bps/Hz, $M^{\text{one}} = 540$ antennas should be employed at each BS of a one-bit system, compared with $M^{\text{conv}} = 150$ antennas at each BS of a conventional system, implying that $\kappa = \frac{M^{\text{one}}}{M^{\text{conv}}} = 3.6$.

The relationship between the number of antennas M^{one} needed by the one-bit MIMO system to perform as well as the conventional MIMO system with M^{conv} antennas is further illustrated in Fig. 4. We numerically find and plot the ratio $\kappa = \frac{M^{\text{one}}}{M^{\text{conv}}}$ needed to achieve $|R_{\text{sum}}^{\text{one}} - R_{\text{sum}}^{\text{conv}}| \leq \epsilon$ for $\epsilon = 10^{-3}$ and different values of M^{conv} . The ratio is around 2.5 at low P_t (or SNR = $\frac{P_t}{\sigma^2}$) values in accordance with Corollary 4, while it increases to 3.79 for $M^{\text{conv}} = 100$ as P_t increases to 20dB, due to reasons discussed in Sec. IV-C. The promising observation is that even at moderate to high SNR values as M^{conv} increases, κ increases at a slower rate and eventually starts to decrease and approach one, because the effect of quantization decreases with M as discussed in Remark 1.

Next we study whether we gain in terms of energy efficiency (EE) when we use one-bit ADCs and DACs instead of FR ADCs and DACs. EE is defined in the downlink as

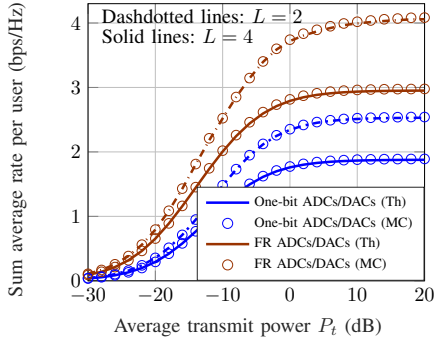


Fig. 2: Sum average rate versus P_t for $M = 128$ and $K = 8$.

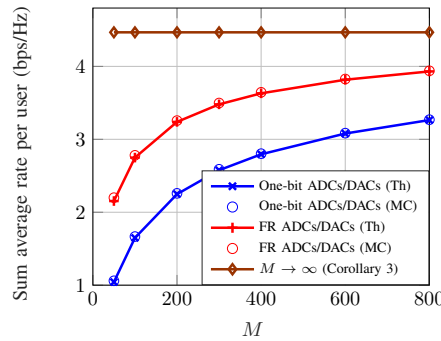


Fig. 3: Sum average rate versus M for $L = 4$, $K = 8$, and $P_t = 10$ dB.

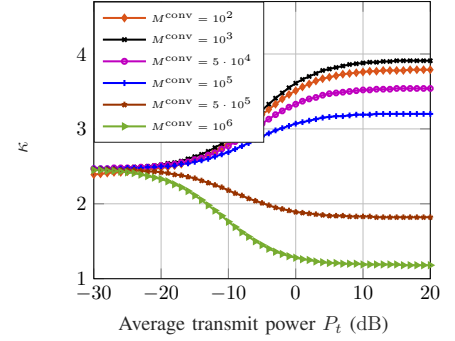


Fig. 4: Ratio $\kappa = \frac{M^{\text{one}}}{M^{\text{conv}}}$ versus P_t for $L = 4$ and $K = 8$.

$EE = \frac{R_{\text{sum}}}{P_{\text{tot}}}$, where $P_{\text{tot}} = \frac{1}{\zeta}P_t + M(2P_{\text{DAC}} + P_{\text{RF}})$, ζ is the power amplifier efficiency, P_{DAC} is the power consumption of each DAC, and P_{RF} is the power consumption per RF chain given in [8]. P_{DAC} scales linearly with the sampling frequency f_s , and exponentially with the number of bits b and is given as $P_{\text{DAC}} = cf_s 2^b$, where $c = 494$ fJ/step/Hz. To compute the EE of conventional massive MIMO cellular system, we consider $M^{\text{conv}} = 128$ antennas at each BS, and assume that each DAC has a resolution of $b = 10$ bits to achieve nearly FR. For the one-bit massive MIMO cellular system, we find that $M^{\text{one}} = 486$ antennas are needed to achieve the same sum average rate as the conventional system. Using this value, we compute $R_{\text{sum}}^{\text{one}}$, P_{tot} with $b = 1$, and consequently the EE. The results are plotted against f_s in Fig. 5. The EE achieved by the one-bit MIMO system exceeds that achieved by the conventional MIMO system for $f_s > 100$ MHz, while achieving the same sum average rate. The decrease in the EE of the conventional system with f_s is significant because the power consumption of FR ADCs and DACs is quite dominant. This is a very promising result especially for mmWave communication systems, that utilize larger bandwidths and higher sampling rates. Thus one-bit massive MIMO is an energy-efficient solution even under linear ZF precoding and imperfect CSI for mmWave systems.

VI. CONCLUSION

This work studied a multi-cell massive MIMO system employing one-bit ADCs and DACs under ZF precoding and imperfect CSI. We derived closed-form expressions of the MMSE channel estimates at each BS and the ergodic achievable downlink rates at the users, utilizing the Bussgang decompositions of the quantized received training and transmit signals respectively. We then studied the ratio of the number of antennas at each BS in the one-bit cellular system to that at each BS in the conventional system required for both systems to achieve the same sum average rate. The ratio turned out to be 2.5 at low SNR, while it was seen to decrease to one for any given SNR as we consider larger antenna arrays. We also observed one-bit MIMO to be more energy efficient than conventional MIMO at higher bandwidths.

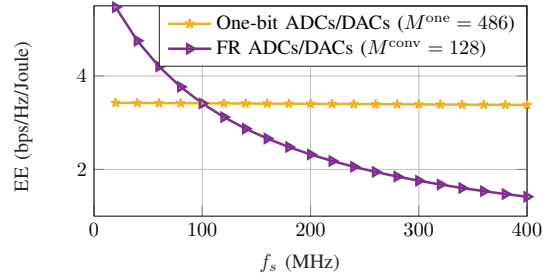


Fig. 5: EE versus the sampling frequency of ADCs/DACs for $L = 4$, $K = 8$ and $P_t = 10$ dB.

REFERENCES

- [1] J. Hoydis, S. ten Brink, and M. Debbah, "Massive MIMO in the UL/DL of cellular networks: How many antennas do we need?" *IEEE J. Sel. Areas Commun.*, vol. 31, no. 2, pp. 160–171, 2013.
- [2] R. Walden, "Analog-to-digital converter survey and analysis," *IEEE J. Sel. Areas Commun.*, vol. 17, no. 4, pp. 539–550, 1999.
- [3] A. K. Saxena, I. Fijalkow, and A. L. Swindlehurst, "Analysis of one-bit quantized precoding for the multiuser massive MIMO downlink," *IEEE Trans. Signal Process.*, vol. 65, no. 17, pp. 4624–4634, 2017.
- [4] Y. Li *et al.*, "Channel estimation and performance analysis of one-bit massive MIMO systems," *IEEE Trans. Signal Process.*, vol. 65, no. 15, pp. 4075–4089, 2017.
- [5] S. Jacobsson, G. Durisi, M. Coldrey, T. Goldstein, and C. Studer, "Quantized precoding for massive MU-MIMO," *IEEE Trans. Commun.*, vol. 65, no. 11, pp. 4670–4684, 2017.
- [6] Y. Li, C. Tao, A. Lee Swindlehurst, A. Mezghani, and L. Liu, "Downlink achievable rate analysis in massive mimo systems with one-bit DACs," *IEEE Commun. Lett.*, vol. 21, no. 7, pp. 1669–1672, 2017.
- [7] Y. Zhang *et al.*, "Rate analysis of cell-free massive MIMO with one-bit ADCs and DACs," in *IEEE International Symposium on Personal, Indoor and Mobile Radio Communications (PIMRC)*, 2019, pp. 1–6.
- [8] E. Balti and B. L. Evans, "A unified framework for full-duplex massive MIMO cellular networks with low resolution data converters," *IEEE Open J. Commun. Soc.*, vol. 4, pp. 1–28, 2023.
- [9] J. J. Bussgang, "Crosscorrelation functions of amplitude-distorted gaussian signals," Res. Lab. Electron., Massachusetts Inst. Technol., Cambridge, MA, USA, Tech. Rep. 216, 1952.
- [10] A. Papoulis and S. U. Pillai, *Probability, Random Variables, and Stochastic Processes*. New York, NY, USA: McGraw-Hill, 2002.
- [11] H. Cramer, *Random Variables and Probability Distributions*, vol. 36. Cambridge, U.K: Cambridge Univ. Press, 2004.
- [12] J. Jose, A. Ashikhmin, T. L. Marzetta, and S. Vishwanath, "Pilot contamination and precoding in multi-cell TDD systems," *IEEE Trans. Wirel. Commun.*, vol. 10, no. 8, pp. 2640–2651, 2011.